Abstract for paper submitted for presentation at 2000 AIAA Joint Propulsion Conference

RAMAN GAS SPECIES MEASUREMENTS IN HYDROCARBON-FUELED ROCKET ENGINE INJECTOR FLOWS

Joseph A. Wehrmeyer, Mechanical Engineering Department, Vanderbilt University
Huu Phuoc Trinh , Space Transportation Directorate, NASA Marshall Space Flight Center
Roy J. Hartfield, Aerospace Engineering Department, Auburn University
Christopher C. Dobson, Space Transportation Directorate, NASA Marshall Space Flight Center
Richard H. Eskridge, Space Transportation Directorate, NASA Marshall Space Flight Center

Summary

Propellent injector development at MSFC includes experimental analysis using optical techniques, such as Raman, fluorescence, or Mie scattering. For the application of spontaneous Raman scattering to hydrocarbon-fueled flows a technique needs to be developed to remove the interfering polycyclic aromatic hydrocarbon fluorescence from the relatively weak Raman signals. A current application of such a technique is to the analysis of the mixing and combustion performance of multijet, impinging-jet candidate fuel injectors for the baseline Mars ascent engine, which will burn methane and liquid oxygen produced in-situ on Mars to reduce the propellent mass transported to Mars for future manned Mars missions. The present technique takes advantage of the strongly polarized nature of Raman scattering. It is shown to be discernable from unpolarized fluorescence interference by subtracting one polarized image from another. Both of these polarized images are obtained from a single laser pulse by using a polarization-separating calcite rhomb mounted in the imaging spectrograph. A demonstration in a propane-air flame is presented.

Introduction

Technology development associated with advanced space transportation propulsion systems includes design and analysis of new types of propellent injectors. An effort exists at NASA-Marshall to include experimentally-obtained reactant/product mixing/combustion information as part of the injector analysis. Hardware associated with this effort includes an optically-accessible high pressure combustion chamber sized for single-element fuel injectors (unielement test article) and a newer, larger modular combustion test article (MCTA) that can accommodate multi-element fuel injector configurations and that is also optically-accessible. Optical accessibility allows laser-based methods, such as laser Mie scattering, fluorescence, and spontaneous Raman scattering, to be applied. Raman spectroscopy has been used to analyze an oxygen-rich gaseous hydrogen/liquid oxygen (GH_2/LOx) injector flow in the unielement test article (1) and most recently is being considered for use in the MCTA to analyze the mixing and combustion performance of multijet, impinging-jet candidate fuel injectors for the baseline Mars ascent engine (2). This engine will burn methane (CH_4) and LOx produced in-situ on Mars to reduce the propellent mass transported to Mars for future manned Mars missions (3).

Application of Raman spectroscopy to hydrocarbon-fueled combustion brings the issue of interference of the weak Raman scattering light signals with strong laser-induced fluorescence. The fluorescence interference can be from polycyclic aromatic hydrocarbons (PAH's) which are excited and fluoresce across the ultraviolet and visible spectrum (4) and when using ultraviolet

lasers can be due to the hydroxyl radical (OH) and to vibrationally-excited O_2, both of which are present in combustion reaction zones (5). By taking advantage of the polarization properties of Raman scattering, it is possible to discriminate the Raman signal from interfering fluorescence interference and hence apply Raman scattering to the analysis of hydrocarbon-fueled combustion. This can be done by obtaining two Raman images, one using a vertically polarized laser and one using a horizontally-polarized laser, and then subtracting the intensity of one image from another to obtain a net Raman signal (6). A second method that lends itself to single-pulse (and hence instantaneous) measurements is to obtain two simultaneous Raman images created from the same laser pulse. One of these images is the vertically-polarized signal and one is for the horizontally-polarized signal. The difference between these images provides the net Raman signal, free of fluorescence interference. This technique has been demonstrated for a time-averaged application (7) and this paper describes a single-pulse application of the technique.

Background

Raman scattering is a weak light scattering process that can be understood by realizing that molecular internal energy can be stored in several modes, including: electronic (quantum mechanical energy level described by the labels *X*, *A*, *B*, etc.), vibration (v = 0, 1, etc.), and rotation (J = 0, 1, etc.), and that light energy is quantized into photons and the energy of each photon is inversely proportional to wavelength. A Stokes Q-branch Raman scattering process involves an absorption of one laser photon at the laser wavelength λ_{LASER} and a subsequent emission of a photon with less energy at a longer wavelength. The Raman wavelength λ_{RAMAN} depends on the vibrational energy level spacing of the laser and hence is different for each molecule. The Raman scattering signals are linearly related to the density of each molecular species and are all relatively weak compared to other light scattering processes, such as Rayleigh scattering and fluorescence. To increase Raman signal strength a UV laser can be used because Raman signal strength for a given laser power increases with a decrease in laser wavelength (5). For the present work a pulsed UV laser, in particular a pulsed, narrowband, tunable KrF excimer laser is used which produces light in a 0.001 nm bandwidth that is tunable from 248 to 249 nm and is pulsed up to 50 Hz with a pulse energy of 400 mJ and a pulse length of 20 nsec. Using a pulsed laser allows rejection of continuous flame emission by gating the light detection system on only during the laser pulse. A narrowband, tunable laser is used to minimize the problem of laser-induced OH and O_2 fluorescence by tuning the laser bandwidth between fluorescence excitation lines (5), at least for atmospheric pressure flames, but for high pressure flames pressure broadening becomes so prevalent that some OH and O_2 is to be expected (1).

Figures 1a and 1b shows simulated Raman spectra, using RAMSES (8) for 300 K reactants in the baseline Mars ascent engine (CH_4 and O_2) for the baseline O/F ratio of 3. Figure 1b shows the expected Raman spectrum at adiabatic equilibrium and a chamber pressure of 250 psia. These spectra show how Raman scattering can reveal both the extent of mixing of propellents near the injector face (by the amount of simultaneous occurrence of CH_4 and O_2) and the extent of reaction (by the relative amounts of reactants and products detected). The signal strength of Raman scattering depends on two molecular invariants, the square of the mean polarizability $(a')^2$ and the square of the anisotropic polarizability $(\gamma')^2$. These are used in an equation for a constant Φ, that can be considered as the Raman scattering cross section for a single molecule. The value of Φ also depends on the polarization of the incident laser beam, the polarization of the detected Raman signal, and the angle of detected Raman signal with respect to

incoming laser beam. For a 90° collection angle and for the Raman and laser beams both in a horizontal plane, the value of Φ for vertically polarized Raman signal is (9):

$$\Phi = (a')^2 + 1/45\ (\gamma')^2$$

and for horizontally polarized Raman signal Φ is:

$$\Phi = 1/60\ (\gamma')^2$$

Usually a'^2 and γ'^2 are similar in magnitude and thus the vertically polarized light is almost two orders of magnitude greater than the horizontally polarized light. Thus the Raman scattering signal essentially retains the polarization of the incoming laser beam. However a fluorescence light emission process does not retain the laser polarization because of the relatively long time the molecule exists in the excited state before fluorescing. During this time the molecule rotates, eliminating any correlation between the polarization of absorbed and emitted photons.

The difference in polarization properties between Raman and fluorescence is exploited in the experimental system shown schematically in Fig. 2. It represents a typical UV Raman system in that a pulsed, narrowband KrF UV laser is used as the light source and an imaging spectrograph coupled to a gated, intensified CCD camera is used as the detection device. The intensifier and laser are triggered simultaneously using a Princeton Instruments PG200 programmable pulser. The laser is focused to a beam waist of 250 μm using a 500 mm focal length lens. The unique feature of this system is the insertion of a calcite rhomb just behind the entrance slit of the spectrograph. This optical element displaces the horizontally polarized Raman image about 5 mm from the vertically polarized Raman image, which travels directly straight through the rhomb. The length of the entrance slit is limited to 4 mm to keep the two polarized images from overlapping. Figure 3 shows a typical single-pulse image obtained from the experimental system, and this image shows the relative strength of vertically polarized signal compared to horizontally polarized signal. The H_2O Raman signal (from air humidity) is almost completely polarized, while the N_2 signal is slightly depolarized and the O_2 signal is more depolarized than N_2. This corresponds to others' experimental observations (6,10).

Spatially-integrated single-pulse Raman spectra are shown in Fig. 4, obtained from a slightly premixed C_3H_8-air bunsen flame. One of these spectra is the vertically polarized Raman-fluorescence signal. The horizontally polarized signal shows essentially only the fluorescence signal, which has two contributions. A broadband component is caused by PAH fluorescence, extending from below 255 nm to above 275 nm. A second contribution to the fluorescence background is the OH fluorescence from about 265 to 270 nm, caused by tuning the laser slightly onto a strong OH transition. This is done to demonstrate the ability of the technique to simultaneously measure Raman spectra and OH fluorescence. Before subtracting the horizontally polarized signal from the vertical it is first multiplied by a factor of 2.22 to account for the ratio in transmission efficiency (for the specctrometer/calcite rhomb) between the vertically and horizontally polarized signals. The net signal shows a fluorescence-free Raman spectrum that shows the simultaneous occurrence of CO_2 and H_2O (products of combustion), CO and H_2 (intermediate products), and unburned C_3H_8. Information about the spatial structure of the flame can be revealed in the single-pulse image of Fig. 5. This image shows unburned C_3H_8 occurring near the 0 mm position. The cooler, denser unburned gas mixture also provides a

stronger N_2 Raman signal near that location. At ~1.5 mm the C_3H_8 pyrolizes into other hydrocarbons, including PAH's that cause a strip of broadband fluorescence to appear at this location. Farther into the flame chemical reactions involving oxidation take place, creating the OH intermediate. This shows up in Fig. 5 by the replacement of PAH fluorescence with OH fluorescence at flame positions greater than ~2.5 mm. By subtracting the scaled upper part of Fig. 5 (horizontally polarized fluorescence signal) from the bottom part (vertically polarized signal), and by summing the net Raman signal for each location (wavelength integration) a qualitative picture of the structure of the flame can be discerned, as in Fig. 6. This figure shows the drop in C_3H_8 signal and the concurrent increase in H_2O signal, showing the formation of that product occurring close to the fuel zone. In the same region the H_2 and CO signals are generally higher than in the fuel zone or in the OH reaction zone past 2.5 mm.

Conclusions

Taking advantage of the strongly polarized nature of Raman scattering, it can be discerned from unpolarized fluorescence interference by subtracting one polarized image from another. Both of these polarized images can be obtained from a single laser pulse by using a polarization-separating calcite rhomb mounted in the imaging spectrograph. This reduces the imaged laser beam length from 12.5 mm down to 4 mm but allows fluorescence-free Raman measurements in propane-air flames. In the pyrolysis zone of these flames considerable PAH fluorescence exists and in a separate flame zone there exists considerable OH fluorescence. However the polarization separation technique is robust enough to allow simultaneous Raman and OH fluorescence measurements to be obtained, which can provide even more information about flame chemical reaction zones.

Most Recent Work

Figure 7 shows an application of the polarization-resolved UV Raman system to the analysis of an actual hot fire test, using liquid methane and Lox. The main stage pressure during the test was 450 psig. The test was associated with injector development for the Mars Ascent Engine program at NASA Marshall.

References

1. Wehrmeyer, J. A., J. M. Cramer, R. H. Eskridge, and C. C. Dobson, "UV Raman Diagnostics for Rocket Engine Injector Development," AIAA Paper 97-2843, 1997.
2. Mueller, P. J., D. W. Plachta, T. Peters, J. C. Whitehead, "Subscale Precursor to a Human Mars Mission Using In-Situ Propellent Production," AIAA Paper 98-3301, 1998.
3. Kos, L., "The Human Mars Mission: Transportation Assessment," Space Technology and Applications International Forum Conference, Abuquerque, N.M., Conference Proceedings Part III, p. 1211, Jan. 1998.
4. Smyth, K., *Combustion and Flame*, 1999.
5. Wehrmeyer, J. A., T.-S. Cheng, and R. W. Pitz, "Raman Scattering Measurements in Flames Using a Tunable KrF Excimer Laser, *Applied Optics* 31: pp. 1495-1504, 1992.
6. Grünefeld, G., V. Beuhausen, and P. Andresen, "Interference-Free UV-Laser-Induced Raman and Rayleigh Measurements in Hydrocarbon Combustion Using Polarization Properties," *Applied Physics B* 61: pp. 473-478.
7. Hartfield, R., C. Dobson, R. Eskridge, and J. Wehrmeyer, "Development of a Technique for Separating Raman Scattering Signals from Background Emission with Single-Shot Measurement Potential," AIAA Paper 97-3357, 1997.
8. Hassel, E. P., "Ultraviolet Raman Scattering Measurements in Flames Using a Narrowband Excimer Laser," Applied Optics 32, 1993.
9. Long, D., "Raman Spectroscopy," McGraw-Hill, 1977.
10. Penney, C. M., L. M. Goldman, M. Lapp, "Raman Scattering Cross Sections," *Nature Physical Science* 235: pp. 110-112.

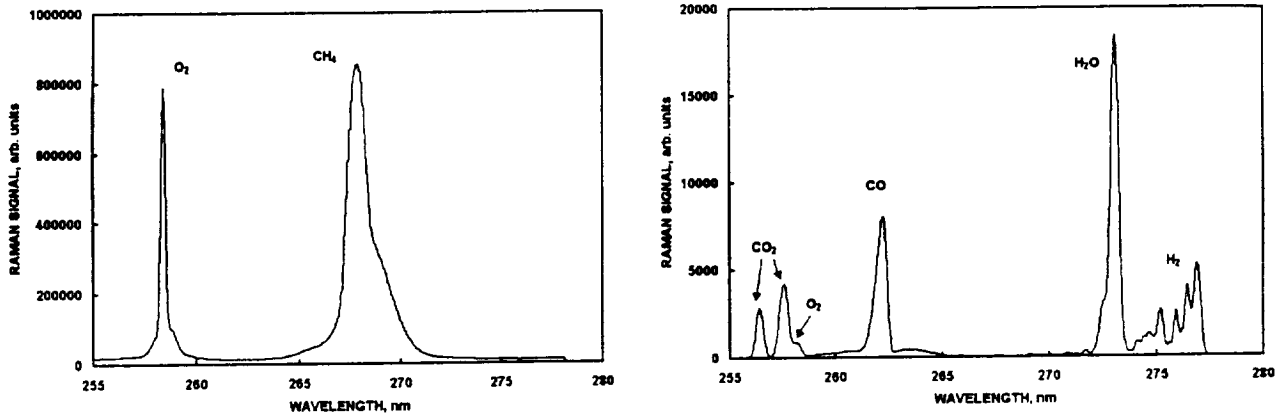

Fig. 1a,b. Simulated Raman spectra using RAMSES for Mars ascent engine baseline conditions: methane/oxygen mass ratio = 3, chamber pressure = 250 psia, adiabatic flame temperature = 3390 K. a (left) 300 K reactants. b(right) completely reacted products.

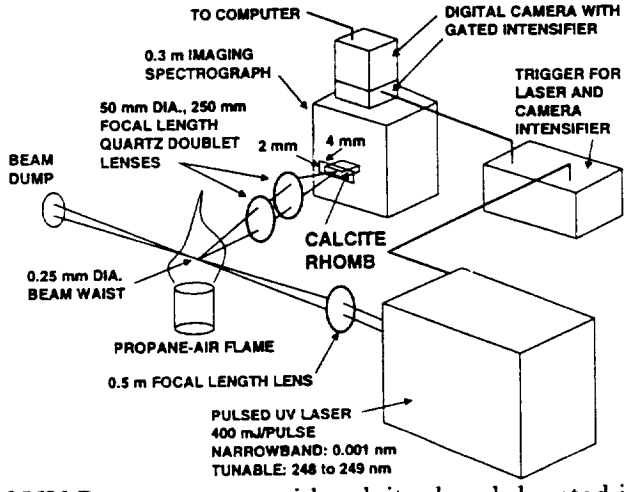

Fig. 2. Schematic of UV Raman system with calcite rhomb located inside imaging spectrograph.

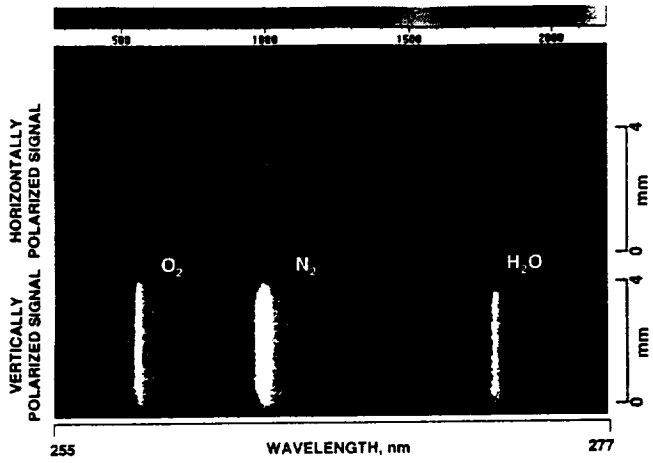

Fig. 3. Single-pulse, polarization-resolved Raman image in humid air.

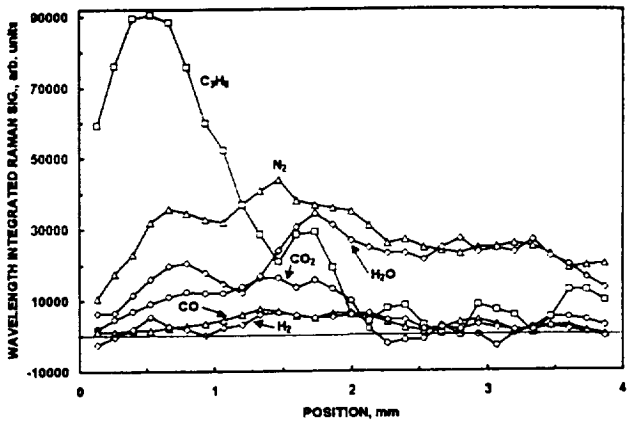

Fig. 6. Net wavelength-integrated Raman signal vs. position for image of Fig. 5.

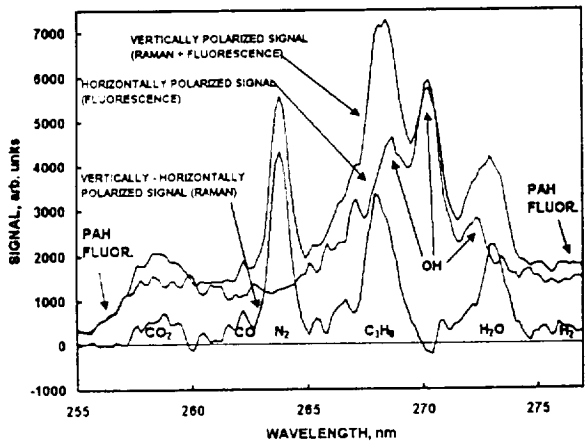

Fig. 4. Single-pulse, polarization-resolved Raman spectra in propane-air flame.

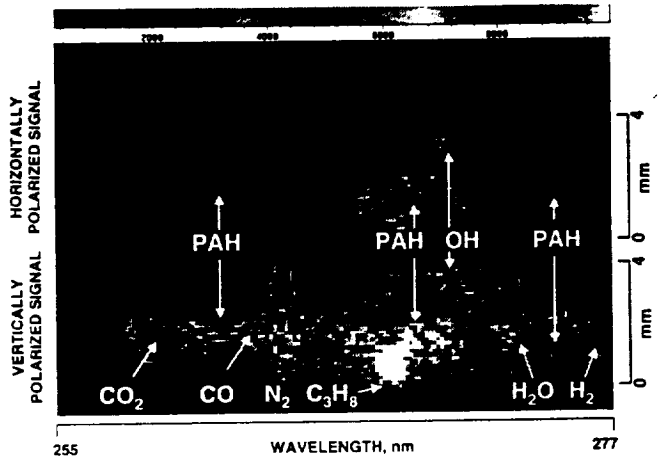

Fig. 5. Single-pulse, polarization-resolved Raman image in propane-air flame.

FIG. 7, SELECTED RAMAN IMAGES FROM CH4-Lox HOT FIRE TEST